Systemic and white adipose tissue inflammation in obesity and insulin resistance

Beek, L. van

3

The limited storage capacity of gonadal adipose tissue directs the development of metabolic disorders in male C57Bl/6J mice

Lianne van Beek, Jan B van Klinken, Amanda CM Pronk, Andrea D van Dam, Eline Dirven, Patrick CN Rensen, Frits Koning, Ko Willems van Dijk, Vanessa van Harmelen

Diabetologia, 2015

Abstract

Aim: White adipose tissue (WAT) consists of various depots with different adipocyte functionality and immune cell composition. Knowledge about WAT depot-specific differences in expandability and immune cell influx during the development of obesity is limited, therefore we aimed to characterize different WAT depots during the development of obesity in mice.

Methods: Gonadal (gWAT), subcutaneous (sWAT) and mesenteric WAT (mWAT) were isolated from male C57Bl/6J mice with different body weights (approximately 25-60 g), analysed, and linear and non-linear regression models were used to describe the extent of WAT depot expandability and immune cell composition as a function of body weight.

Results: Whereas mouse sWAT and mWAT remained expanding with body weight, gWAT expanded mainly during the initial phase of body weight gain, after which the expansion diminished around a body weight of 40 grams. From this point on, gWAT crown-like structure formation, liver steatosis and insulin resistance occurred. Mouse WAT depots showed major differences in immune cell composition; gWAT mainly consisted of macrophages, whereas sWAT and mWAT contained primarily lymphocytes.

Conclusion: Marked inter-depot differences exist regarding WAT immune cell composition and expandability. The limited storage capacity of gWAT seems to direct the development of metabolic disorders in male C57Bl/6J mice.

Introduction

White adipose tissue (WAT) is the main energy storage organ, which is distributed over various depots. Regional distribution and inflammatory status of WAT are strongly associated with the development of metabolic disorders. Excessive abdominal fat, or central obesity, is known as a strong risk factor for type 2 diabetes mellitus and cardiovascular disease (1, 2). WAT can be divided into subcutaneous WAT (sWAT) and visceral WAT (vWAT), located underneath the skin and around the abdominal organs, respectively. Mouse vWAT is generally subdivided into mesenteric WAT (in between the organs; mWAT) and gonadal WAT (around the testes; gWAT). While WAT was originally considered as an organ with homogeneous function, vWAT is now thought to exert more adverse effects on health as compared to sWAT (2-4). These pathophysiological differences in WAT depots are linked to the metabolic and inflammatory status of the tissue.

Due to excessive fat accumulation in WAT during obesity, adipocytes become stressed and release increased amounts of fatty acids and pro-inflammatory adipokines and chemokines. These inflammatory signals induce immune cell infiltration and dysfunction of the obese WAT (5-7). Macrophage accumulation or more specifically the presence of crown-like structures (CLS) in the WAT is associated with adipocyte death caused by cellular lipid overload (8, 9). Furthermore, T and B lymphocytes are increased in WAT during obesity and do contribute to the development of metabolic disorders (10, 11). Pro-inflammatory cytokines produced by both adipocytes and infiltrated immune cells directly interfere with the insulin signalling pathway, thereby affecting insulin sensitivity both locally and systemically, leading to insulin resistance (IR) and type 2 diabetes (12, 13). vWAT as compared to sWAT secretes more fatty acids and pro-inflammatory cytokines and has a higher infiltration of cytotoxic T cells and macrophages during obesity (14-16).

Most of the human studies on WAT inflammation compare WAT between lean and obese individuals and considered only one WAT depot. The majority of mouse studies use male C57Bl/6J mice as a model to induce obesity by a high fat diet and assess only the gWAT whereas the sWAT and mWAT are being neglected (17). As different WAT depots have different function and cellular composition, it is of importance to determine the functional and immunological phenotypes of the various WAT depots. Moreover, longitudinal studies following the development of obesity are sparse and as a consequence the inflammatory response of the different WAT depots during body weight gain has until now being poorly characterized. Therefore, the aim of the current study was to phenotype the different WAT depots and to determine regional differences with regard to WAT expandability and inflammation in male C57Bl/6J mice during the development of high fat diet (HFD) induced obesity. In addition, we set out to develop a set of linear and non-linear regression models to describe organ weights and WAT (immune cell) composition as a function of body weight.

Materials and methods

Animals

Experiments were performed with six different batches male C57Bl/6J mice (Charles River, Maastricht, The Netherlands). The batches differed in duration (4-34 weeks) and type of HFD (45% or 60% energy derived from lard fat; D12451 or D12492, Research Diet Services, Wijk bij Duurstede, The Netherlands) (ESM Table 1). Body weight was measured and lean and fat mass was assessed by MRI based body composition analysis (Echo MRI, Echo Medical Systems, USA). At the end of the diet intervention, mice were sacrificed, perfused, and organs were dissected for further analysis. All experiments were approved by the animal ethics committee of Leiden University Medical Center.

Adipocyte and stromal vascular cell isolation

gWAT (one side), sWAT (posterior, one side) and mWAT depots of the mice were dissected and kept in PBS after diet intervention. Tissues were processed for adipocyte size determination as previously described (18). Adipocyte number per fat pad was calculated from the fat pad mass and adipocyte size. The residue of the WAT filtrate was used for the isolation of stromal vascular fraction (SVF) to analyse immune cell composition using flow cytometry. After centrifugation (350 x g, 10 minutes) the supernatant was discarded and the pellet was treated with erythrocyte lysis buffer after which the cells were counted using an automated cell counter (TC10, Biorad, CA, USA). The SVF was fixed using 0.5% paraformaldehyde, stored in FACS buffer (PBS, 0.02% sodium azide, 0.5% FCS) in the dark at 4°C and analysed within one week.

Additional analyses

Plasma, liver TG, adipocytes lipolysis, histology, and flow cytometry analysis are performed as described in the ESM methods.

Statistics

Data are presented as single data points, or mean ± SD. Statistical differences between groups were calculated with the student's t-test using GraphPad Prism version 6 (GraphPad software, CA, USA). Correlation analyses were performed by making correlation plots of body weight versus the various parameters measured in this study. We modelled the association between each variable and body weight using regression assuming either a linear ($y=b*x+c$; $a=1$) or non-linear power function. The non-linear power functions could either have y-intercept ($y=b*x^a+c$; $a>1$, exponential form), or x-intercept ($y=b*(x-c)^a$; $a<1$, curve tapering off); x=body weight, y=lean, fat or individual organ mass. For each analysis the p-value zero slope (p) indicated if the slope was significantly different from zero (b=0, horizontal line). In addition, superiority of the non-linear (power) function over the linear model was determined by testing the hypothesis $a=1$ using the extra sum-of-squares F test; the corresponding p-value was termed p-value linear indicated by p*. A Spearman rank correlation coefficient (r) was determined for every association. $P<0.05$ was considered statistically significant, unless stated otherwise after Bonferroni multiple test correction, significant values in the tables are shown in bold.

Results

HFD-induced changes in body composition and organ weight.

C57Bl/6J mice were subjected to different diet interventions, for a variable number of weeks and with a varying fat percentage in the diet to be able to study mice with a broad range of body weight, ranging from lean to severely obese (26.3-59.3 g, n=54). The fat percentage of lean mice (<30 g) consisted of about 80% lean mass and 20% fat mass. Mice exposed to HFD increased both lean and fat mass, although fat mass increased relatively more (Figure 1A,B; ESM Table 2). Obese mice consisted of up to 50% fat mass. Figure 1C shows that the liver weight increased non-linearly with a power >1 when correlated to body weight, with a substantial increased liver weight from approximately 40 grams on. This was mainly caused by an increase of fat in the liver (ESM Figure 1A). Also heart weight had a non-linear correlation with body weight (Figure 1D). Spleen weight correlated linearly with body weight (Figure 1E), even as brown adipose tissue (BAT) which showed a very strong linear positive correlation with body weight (Figure 1F). BAT lipid droplet content correlated positively both with body weight (ESM Figure 1B) and BAT weight ($r=0.64$, $p=0.0001$, data not shown). ESM Table 2 shows the equations of the curves of the correlations between the individual organs and body weight after best fit comparison statistics. Plasma glucose and insulin as well as plasma lipid levels were measured and correlated with body weight. Glucose increased at the start of body weight gain, after which it tapered off (Figure 2A). As glucose levels are regulated by insulin, the flattening of the glucose curve can be linked to increasing insulin levels (Figure 2B). Plasma total cholesterol correlated positively with body weight ($r=0.72$, $p<0.0001$), whereas other plasma lipids (triacylglycerol (TG) and non-esterified fatty acid) were not correlating with body weight (data not shown).

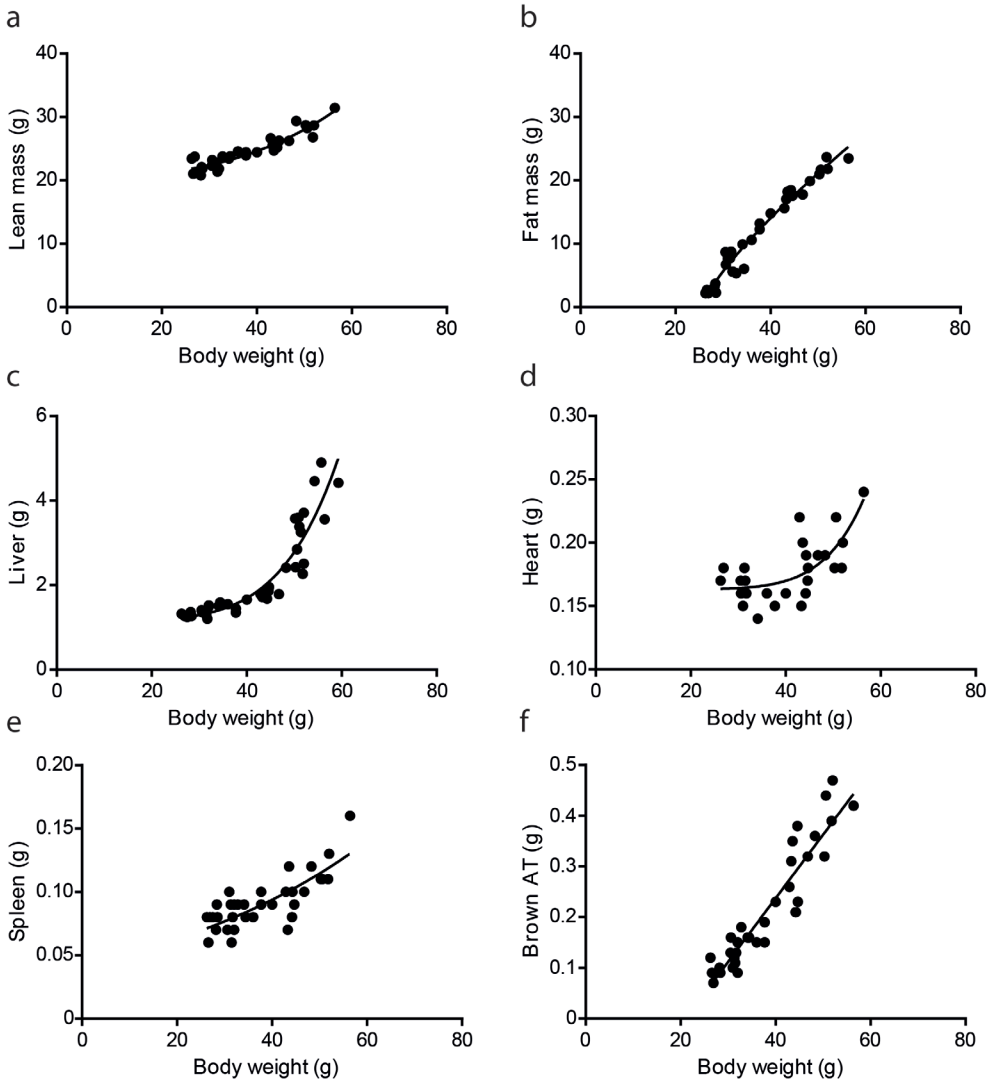

Figure 1. HFD-induced changes in body composition and organ weight in correlation to body weight. Correlations are shown between lean mass (A), fat mass (B) and different organ weights; liver (C), heart (D), spleen (E), and interscapular BAT (F) with body weight of male C57Bl/6J mice (ranging from approximately 25-60 grams). Correlations were determined by fitting a linear model or non-linear power function, 95% confidence interval is shown as grey bands, see ESM Table 2 for equations, correlations and p-values.

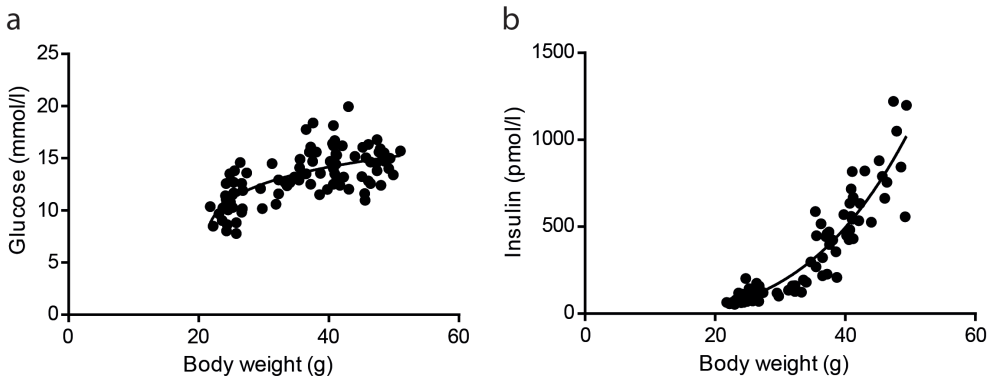

Figure 2. HFD-induced changes in glucose and insulin plasma levels in correlation to body weight. The correlation between glucose (A; r=0.67, p<0.0001, p*=0.0044) and insulin (B; r=0.93, p<0.0001, p*<0.0001) plasma levels with body weight of male C57Bl/6J mice. Correlations were determined by fitting a linear model or non-linear power function, 95% confidence interval is shown as grey bands. A significant value of p provides evidence of a non-zero slope in the linear model; a significant value of p* provides evidence that the association in non-linear

Expandability of mouse WAT depots.

Fat pad weight of the various WAT depots reflects expandability during HFD exposure. The gWAT depot expanded mostly during the initial phase of weight gain compared to both sWAT and mWAT. With progressing weight gain, the gWAT growth curve tapered off, whereas sWAT and mWAT remained growing with body weight (Figure 3A,C,E; ESM Table 2). This is also illustrated by ESM Figure 2, where mice were divided into groups based on body weight to determine the adipocyte size distribution. Whereas for both sWAT and mWAT the adipocyte size distribution curve shifted towards larger adipocytes with higher body weight, gWAT adipocytes remained comparable in size from approximately 40 grams onwards. Interestingly, the gonadal adipocytes were larger compared to adipocytes of sWAT and mWAT, for both lean and obese mice (Figure 3B,D,F; ESM Table 3A,B). The potency of insulin to inhibit lipolysis in gonadal adipocytes was tested ex vivo and revealed a negative correlation with body weight (Figure 4A), as well as with adipocyte size (r=-0.42, p=0.0043, data not shown). WAT growth is accomplished by hypertrophy (increase in size) or hyperplasia (increase in number) of the adipocytes. For all three WAT depots, there was a significant correlation between body weight and adipocyte size (Figure 3B,D,F; Table 1) whereas adipocyte number did not correlate with body weight (Table 1). However, when correlated with WAT depot weight, adipocyte number did show a slight positive correlation for gWAT and mWAT (data not shown). These data indicate that WAT expansion occurred predominantly by adipocyte hypertrophy and somewhat by hyperplasia in gWAT and mWAT, whereas sWAT only expanded by adipocyte hypertrophy.

Table 1. WAT depot composition correlated to body weight of mice on a HFD

	Correlation to body weight - Statistics					
	a	b	c	r	P-value zero slope	P-value linear
Gonadal WAT						
Adipocyte size (µm; n=54)	0.1482	78.63	25.46	0.8112	1.40E-19***	2.92E-07***
Adipocyte no/fat pad (n=46)				0.1822	3.773	-
SVF nr/fat pad (n=54)	1	40,829	-672,214	0.6768	1.20E-05***	5.282
Leukocytes (% CD45 of SVF; n=44)	1	0.5060	42.98	0.4131	0.1197	-
T lymphocytes (% CD3 of SVF; n=44)	1	0.2878	0.1631	0.3518	0.0315*	-
T lymphocyte ratio (CD4:CD8; n=51)	1	-0.1689	10.71	-0.6287	7.28E-05***	0.8226
B lymphocytes (% CD19 of SVF; n=35)	1	0.1398	-1.206	0.3631	0.0963	-
Macrophages (% F4/80 of SVF; n=50)				-0.1962	3.834	-
Macrophage ratio (M1:M2; n=45)	1	0.01534	- 0.3574	0.7710	7.92E-08***	8.699
Subcutaneous WAT						
Adipocyte size (µm; n=54)	0.2473	49.44	24.39	0.8886	3.26E-20***	4.33E-04***
Adipocyte no/fat pad (n=46)				-0.03627	7.093	-
SVF nr/fat pad (n=54)				0.2907	1.252	-
Leukocytes (% CD45 of SVF; n=50)	1	0.6146	32.41	0.4680	0.0036**	4.694
T lymphocytes (% CD3 of SVF; n=40)				0.1068	8.776	-
T lymphocyte ratio (CD4:CD8; n=50)	1	-0.03013	2.784	-0.4064	0.1818	-
B lymphocytes (% CD19 of SVF; n=43)				-0.07501	4.874	-
Macrophages (% F4/80 of SVF; n=29)				-0.1822	5.057	-
Macrophage ratio (M1:M2; n=34)	1	0.01025	- 0.2255	0.6262	1.95E-06***	0.5508
Mesenteric WAT						
Adipocyte size (µm; n=54)	0.3524	34.09	22.17	0.9528	3.17E-29***	3.23E-04***
Adipocyte no/fat pad (n=46)				-0.06658	5.114	-
SVF nr/fat pad (n=54)				0.1914	2.070	-
Leukocytes (% CD45 of SVF; n=49)	1	-0.6190	97.37	-0.3613	0.0729	-
T lymphocytes (% CD3 of SVF; n=48)	1	-0.7400	54.93	-0.6355	7.07E-06***	0.5445
T lymphocyte ratio (CD4:CD8; n=48)				0.06193	3.512	-
B lymphocytes (% CD19 of SVF; n=30)	1	-0.9100	72.53	-0.3696	0.0261	-
Macrophages (% F4/80 of SVF; n=23)	1	0.9423	-22.89	0.5198	0.0153*	0.1161
Macrophage ratio (M1:M2; n=29)	1	0.01035	- 0.2701	0.6768	6.93E-04***	0.2763

P<0.0019 is considered statistically significant after Bonferroni multiple test correction.

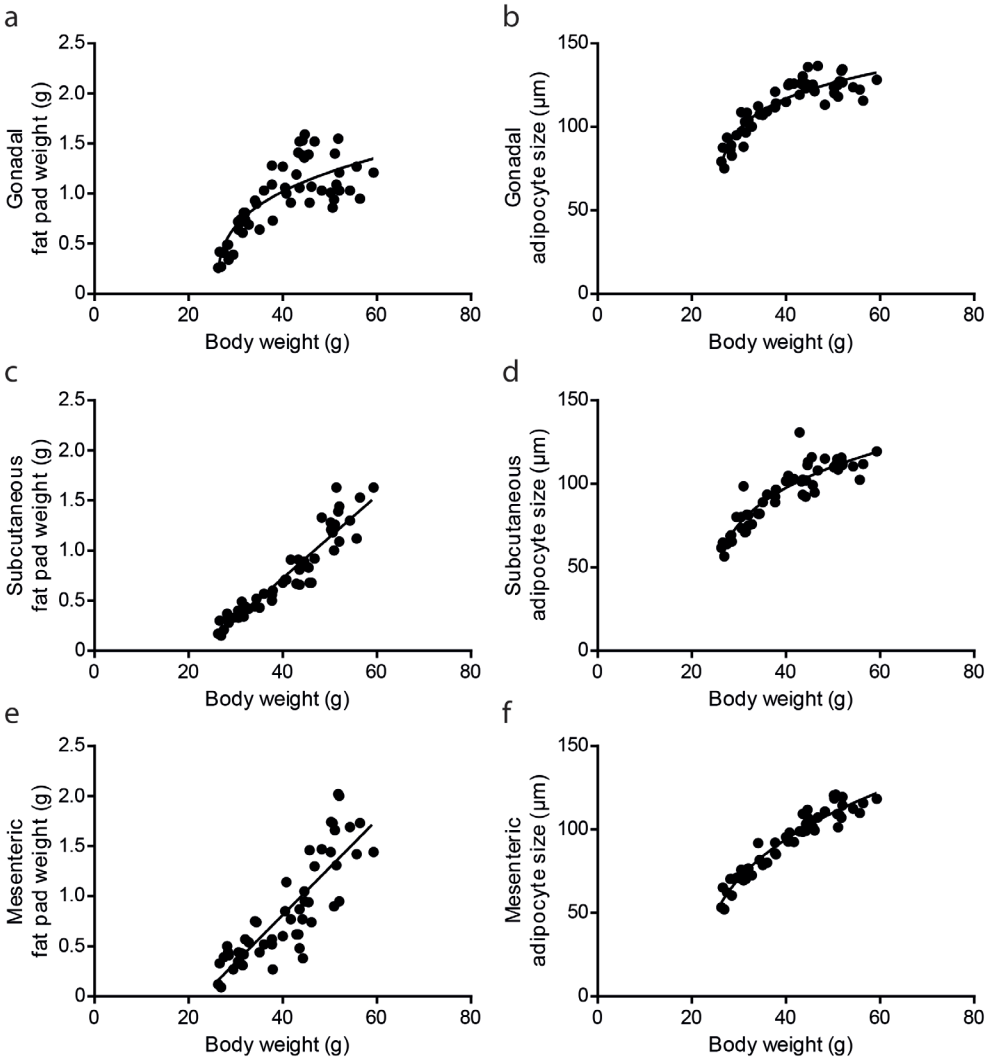

Figure 3. HFD-induced changes in fat pad weight and adipocyte size in correlation to body weight. Fat pad weight (A, C, E) and adipocyte size (B, D, F) of gWAT, sWAT and mWAT in correlation to body weight of male C57Bl/6J mice. For gWAT and sWAT one fad pad is used for representation. Correlations were determined by fitting a linear model or non-linear power function, 95% confidence interval is shown as grey bands, see Table 1 and ESM Table 2 for equations, correlations and p-values.

HFD-induced changes in immune cell composition in mouse WAT depots.

WAT depots were processed to isolate the SVF, which contains immune cells as well as pre-adipocytes and endothelial cells. The absolute SVF cell number was determined and represented per fat pad. The SVF cell count of gWAT correlated positively with body weight, whereas the SVF cell counts of sWAT and mWAT did not correlate with body weight (Table 1). Absolute leukocyte numbers (CD45+ cells) per fat pad showed a linear correlation with body weight for both gWAT and sWAT, whereas leukocyte

numbers in mWAT showed no correlation with body weight (ESM Figure 3A, 4A, 5A). Absolute T cell numbers of gWAT and sWAT, but not mWAT correlated positively with body weight (ESM Figure 3B, 4B, 5B). Within the T cell population, the ratio between T helper cells and cytotoxic T cells (CD4+ and CD8+ cells, respectively) was determined. In both gWAT and sWAT the CD4:CD8 ratio showed a negative correlation with bodyweight, which indicates a relative larger increase in cytotoxic T cells compared to T helper cells (Table 1). Absolute B cell numbers (CD19+ cells) showed a positive correlation with body weight for gWAT (ESM Figure 4D).

Absolute macrophage numbers (F4/80+ cells) of all three WAT depots correlated positively with body weight (ESM Figure 3C, 4C, 5C). Interestingly, absolute macrophage numbers in gWAT and sWAT showed a non-linear correlation with body weight with a power >1, while the correlation in mWAT was linear. WAT macrophages can form CLS, which is shown in Figure 4B by F4/80 staining of gWAT. CLS increased non-linearly with increasing body weight with a power >1 in the gWAT depot (Figure 4C). Within the F4/80+ cell population, M1 and M2 macrophages were distinguished using CD11B and CD11C markers (M1: CD11B+CD11C+; M2: CD11B+CD11C-). Figure 4D shows the correlation of M1 and M2 macrophages as percentage of F4/80 cells from the gWAT depot (representative for the other two depots, data not shown) to body weight. Within all AT depots, M1 macrophages were positively correlated and M2 macrophages were negatively correlated with body weight. The M1:M2 ratio also showed a strong positive correlation with body weight within all WAT depots (Table 1). This indicates relatively more M1 macrophages in WAT with a higher body weight. Thus, HFD induces immune cell compositional changes in all three WAT depots, with an increase in immune cell numbers in mainly gWAT and sWAT.

Immune cell composition of distinct WAT depots from lean and obese mice.

gWAT, sWAT and mWAT depots from either lean or obese mice (mean body weight 31.0±2.9 g, n=10 and 50.1±3.6 g, n=8, respectively) were analysed and compared with each other to determine differences in immune cell composition between the adipose tissue regions. In lean mice, approximately 60% of the SVF from gWAT and sWAT consisted of leukocytes (57.5±9.9% and 62.7±6.2%, respectively), and in mWAT this percentage was even higher (78.3±12.1%) (ESM Table 3A). In obese mice, there were no differences in leukocyte percentages in the SVF between the different WAT depots (approximately 65%, ESM Table 3B). T cells were present in all three WAT depots. Interestingly, in mWAT from lean mice the percentage of T cells in the SVF was significantly higher as compared to gWAT and sWAT (ESM Table 3A). The CD4:CD8 ratio in lean sWAT and mWAT was between 1 and 2, which indicates slightly more CD4 cells over CD8 cells. However, lean gWAT contained even more CD4 than CD8 cells as the ratio was around 5 (ESM Table 3A). In obese mice, there were no differences in T cell percentages between the WAT depots (ESM Table 3B). There were major differences in B cell content between the depots ranging from hardly any B cells in gWAT to approximately 35% of the SVF in mWAT of lean mice and approximately 20% of the SVF in mWAT of obese mice (ESM Table 3A,B). gWAT predominantly contained macrophages (approximately 30% of SVF both in lean and obese mice), while less than 10%

of the SVF from sWAT consisted of macrophages in both lean and obese mice. These data indicate that there are large immune cell composition differences between different WAT depots from both lean and obese mice.

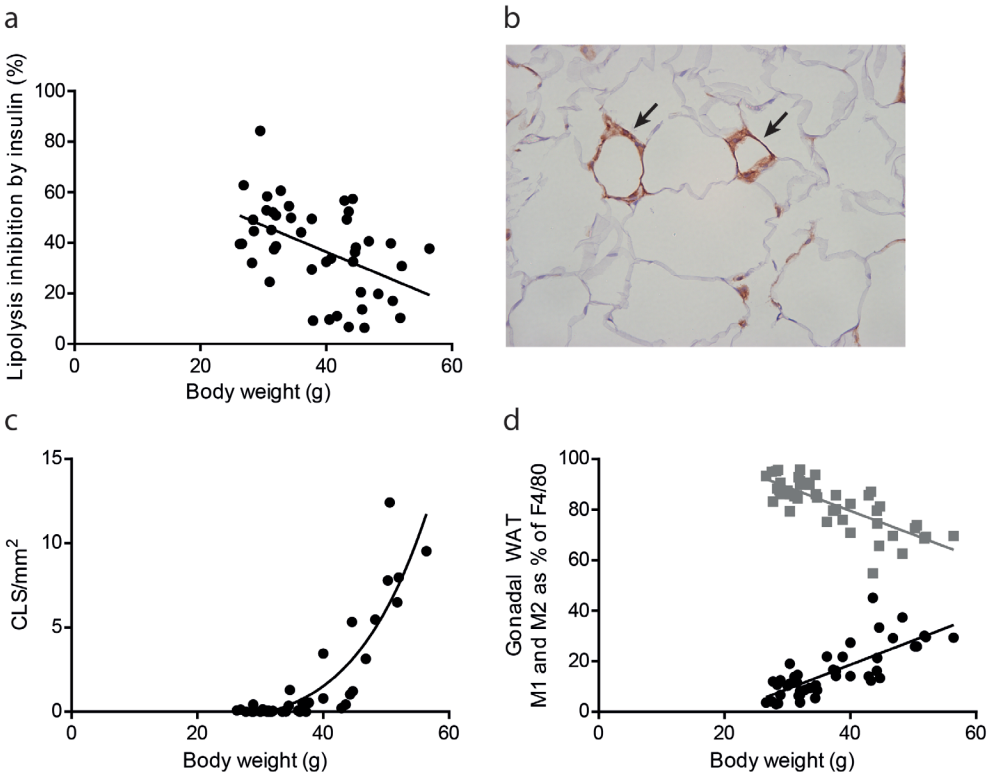

Figure 4. Insulin responsiveness of adipocytes and macrophage phenotype in gWAT in correlation to body weight. Percentage inhibition of lipolysis by insulin of gonadal adipocytes correlated with body weight (A; r=-0.47, p=0.0010). Insulin responsiveness of the adipocytes was determined by measuring the response of the adipocytes to 8-bromo-cAMP stimulated lipolysis and the percentage inhibition thereof by insulin. F4/80 stained macrophages in gWAT (B), CLS are indicated by an arrow. CLS counts per mm^2 WAT correlated with body weight of male C57Bl/6J mice (C; r=0.71, p<0.0001, p*<0.0001). Macrophage type 1 (CD11B+CD11C+; black dots; r=0.77, p<0.0001) and 2 (CD11B+CD11C-; grey dots; r=-0.76, p<0.0001) as percentage of F4/80+ cells in SVF of gWAT by flow cytometry (D) correlated to body weight of male C57Bl/6J mice. Correlations were determined by fitting a linear model or non-linear power function, 95% confidence interval is shown as grey bands. A significant value of p provides evidence of a non-zero slope in the linear model; a significant value of p* provides evidence that the association in non-linear.

Discussion

In the current study we determined intra-depot differences in WAT immune cell composition in relation to WAT expandability. Mouse WAT depots showed major differences in expandability and immune cell infiltration during the development of obesity. Furthermore, a body weight of approximately 40 grams emerged as a critical tipping point from where on metabolic dysfunction occurs, at least in male C57Bl/6J mice. In this paper, we also provide a set of parameterized linear and non-linear functions which can be used by researchers in the field of obesity to assess the extent of WAT depot expansion and inflammation in HFD fed male C57Bl/6J mice as a function of body weight.

It has extensively been shown that distinct WAT depots from both mice and humans feature different metabolic functions. This is due to intrinsic differences in adipocyte characteristics but has also been attributed to differences in immune cell composition in the various depots (19-21). Here, we have performed a direct comparison of the different WAT depots in male C57Bl/6J mice and focussed on the expandability and immune cell composition simultaneously during the development of obesity, which has until now being poorly characterized. Our data confirm great variability in immune cell composition between WAT depots. The characteristics of the different mouse WAT depots already differed in the lean state, and each depot responded differently to body weight gain with respect to immune cell composition as well as expandability. Mouse gWAT expanded mostly during the initial phase of body weight gain, and increased less after a body weight of around 40 grams. Although sWAT and mWAT did not primary expand as fast as gWAT, they both remained expanding with a body weight after 40 grams. This implies that gWAT is the primary storage depot that grows initially in HFD-induced obesity, followed by sWAT and mWAT. This is also reflected by the larger gWAT adipocytes during both the lean and obese state, which has similarly been identified by Sachmann-Sala et al. albeit only in lean mice (22).

Around a body weight of 40 grams where the gWAT growth curve tapered off, the liver started to grow significantly, which is mainly caused by an increase in fat content. Apparently, the gWAT adipocytes were saturated and could not grow any larger to store additional fat. As a consequence, the excess fat which could not be stored in the gWAT depot led to ectopic fat storage in the liver (23). Moreover, around this point of body weight gain, the number of CLS started to increase in the gWAT. As CLS are found around stressed and dying adipocytes (9), the rise in numbers of CLS around 40 grams of body weight appear associated with increased adipocyte death. Also, insulin levels increased substantially from this point on, indicating the development of insulin resistance. Our data therefore imply that approximately 40 grams body weight of male C57Bl/6J mice is an important tipping point from where on WAT and systemic metabolic dysfunction occur concomitantly. In this study, data has been exclusively obtained from male C57Bl/6J mice in combination with HFD to induce obesity. Whether females, other mouse strains / models or humans also have such a threshold BMI upon which WAT inflammation and metabolic dysfunction rapidly increase, remains to be investigated.

Our data are in agreement with the study of Strissel et al., that also showed that at a certain body weight in mice gWAT stops expanding due to increased adipocyte death, whereas liver starts

accumulating fat (24). Strikingly, while our data showed a constant gWAT weight and continuous increase of CLS, they showed a reduction of both gWAT weight and CLS formation after a body weight of 40 grams. This was accompanied by a reduction in adipocyte size and increased adipocyte numbers, which they attributed to newly differentiated adipocytes. One explanation for their findings might be the fact that they fed their mice a 60% HFD for 20 weeks, which may be a more extreme intervention than the interventions used in our study. There are several other studies elucidating regional differences regarding WAT growth (25-27), although these studies do not extensively link WAT expandability to immune cell infiltration and metabolic characterization. This study is the first that focusses on all these processes simultaneously.

Adipocyte size of all three WAT depots increased during body weight gain. Adipocyte number per fat pad remained comparable in all depots when correlated to body weight, whereas in gWAT and mWAT adipocyte numbers increased slightly during the HFD intervention when correlated with fat pad weight. Our observations are in line with previous mouse studies that showed expansion by hypertrophy only in sWAT, whereas mWAT expanded by both hypertrophy and hyperplasia (25, 27). Adipocytes in gWAT were larger as compared to sWAT and mWAT in mice. Large adipocytes are thought to release more pro-inflammatory cytokines and chemokines which attract circulating monocytes into the WAT that in turn differentiate into macrophages (5, 28). Indeed, the SVF of the gWAT contained a higher fraction of macrophages compared to sWAT and mWAT. Also, the absolute number of macrophages per WAT depot was higher in the gWAT than in the other WAT depots.

Absolute leukocyte numbers in mouse mWAT were much higher compared to sWAT and gWAT. mWAT surrounds the intestine, which represents the first line of defence against intestinal pathogens and could therefore explain the large number of leukocytes. However, mWAT is also known to contain a large amount of lymphoid tissue including lymph nodes and milky spots (29). Although we took great care in removing all visible lymph nodes from the mWAT before the immune cell characterization, we cannot exclude the possibility that we missed some lymph nodes. As lymph nodes contain numerous leukocytes, this could also explain the high number of leukocytes present in mouse mWAT. Another issue affecting analyses of WAT inflammation, might be contamination of the SVF with immune cells from the circulation. However, our mice were perfused before removal of the WAT depots.

Numerous pathophysiological processes are known to be associated with the development of IR. In this study, we focussed on WAT expandability and inflammation as a measure for WAT dysfunction. However, inadequate angiogenesis and related hypoxia are known as early determinants for WAT dysfunction as well (30, 31), and can induce WAT fibrosis which has also been associated with IR (32). Although beyond the scope of the current study, it is interesting to determine the association between these pathologies, WAT expansion and inflammation. Macrophages are highly abundant in WAT, with specifically M1 macrophages accumulating during obesity and contributing to IR. Our data showed a phenotypic switch from M2 to M1 type macrophages during obesity, which has previously also been shown by Lumeng et al. (17). CLS numbers increased as well with body weight, which are primarily formed by M1 macrophages (33). M1 macrophages are known to accumulate lipids and form foam

cells. Lipid accumulation in macrophages has previously directly been related to the expansion of WAT (34). Whether lipid loaded macrophages are a consequence of the limited expansion of WAT remains to be investigated.

BAT is known to be a prominent player in body weight control, as it burns TG to produce heat (35, 36). Here we show that BAT weight is strongly correlated to body weight. In general, high BAT weight is associated with inactive BAT, as TG is being stored instead of being used for heat production (37). This is supported by an increased lipid droplet content in BAT with higher body weight. Our observed correlation between BAT weight and body weight can be explained by the thermal insulation function of WAT. The increased WAT in obesity is enough to keep the animal warm and heat production by BAT activity is reduced. Thus, body weight is an important confounder when studying BAT activity.

We conclude that mouse WAT depots vary considerably in expandability and immune cell composition during HFD induced body weight gain. With a body weight threshold of approximately 40 grams in mice, gWAT seems to have reached its maximum expansion capacity and at this point WAT dysfunction and concomitant systemic metabolic dysfunction will commence.

Acknowledgements

The authors would like to thank T.C.M. Streefland (Department of Medicine, Division of Endocrinology, LUMC, The Netherlands) for excellent technical assistance.

Reference list

1. Lee MJ, Wu Y, Fried SK. Adipose tissue heterogeneity: implication of depot differences in adipose tissue for obesity complications. Molecular aspects of medicine. 2013;34(1):1-11.
2. Despres JP, Lemieux I. Abdominal obesity and metabolic syndrome. Nature. 2006;444(7121):881-7.
3. Bjorndal B, Burri L, Staalesen V, Skorve J, Berge RK. Different adipose depots: their role in the development of metabolic syndrome and mitochondrial response to hypolipidemic agents. Journal of obesity. 2011;2011:490650.
4. Tran TT, Yamamoto Y, Gesta S, Kahn CR. Beneficial effects of subcutaneous fat transplantation on metabolism. Cell metabolism. 2008;7(5):410-20.
5. Xu H, Barnes GT, Yang Q, Tan G, Yang D, Chou CJ, et al. Chronic inflammation in fat plays a crucial role in the development of obesity-related insulin resistance. The Journal of clinical investigation. 2003;112(12):1821-30.
6. Hotamisligil GS. Inflammation and metabolic disorders. Nature. 2006;444(7121):860-7.
7. van Beek L, Lips MA, Visser A, Pijl H, Ioan-Facsinay A, Toes R, et al. Increased systemic and adipose tissue inflammation differentiates obese women with T2DM from obese women with normal glucose tolerance. Metabolism: clinical and experimental. 2014;63(4):492-501.
8. Murano I, Barbatelli G, Parisani V, Latini C, Muzzonigro G, Castellucci M, et al. Dead adipocytes, detected as crown-like structures, are prevalent in visceral fat depots of genetically obese mice. Journal of lipid research. 2008;49(7):1562-8.
9. Cinti S, Mitchell G, Barbatelli G, Murano I, Ceresi E, Faloia E, et al. Adipocyte death defines macrophage localization and function in adipose tissue of obese mice and humans. Journal of lipid research. 2005;46(11):2347-55.
10. Winer DA, Winer S, Shen L, Wadia PP, Yantha J, Paltser G, et al. B cells promote insulin resistance through modulation of T cells and production of pathogenic IgG antibodies. Nature medicine. 2011;17(5):610-7.
11. Wu H, Ghosh S, Perrard XD, Feng L, Garcia GE, Perrard JL, et al. T-cell accumulation and regulated on activation, normal T cell expressed and secreted upregulation in adipose tissue in obesity. Circulation. 2007;115(8):1029-38.
12. Hotamisligil GS, Shargill NS, Spiegelman BM. Adipose expression of tumor necrosis factor-alpha: direct role in obesity-linked insulin resistance. Science. 1993;259(5091):87-91.
13. Shoelson SE, Lee J, Goldfine AB. Inflammation and insulin resistance. The Journal of clinical investigation. 2006;116(7):1793-801.
14. Chau YY, Bandiera R, Serrels A, Martinez-Estrada OM, Qing W, Lee M, et al. Visceral and subcutaneous fat have different origins and evidence supports a mesothelial source. Nature cell biology. 2014;16(4):367-75.
15. Vatier C, Kadiri S, Muscat A, Chapron C, Capeau J, Antoine B. Visceral and subcutaneous adipose tissue from lean women respond differently to lipopolysaccharide-induced alteration of inflammation and glyceroneogenesis. Nutrition & diabetes. 2012;2:e51.
16. Bigornia SJ, Farb MG, Mott MM, Hess DT, Carmine B, Fiscale A, et al. Relation of depot-specific adipose inflammation to insulin resistance in human obesity. Nutrition & diabetes. 2012;2:e30.
17. Lumeng CN, Bodzin JL, Saltiel AR. Obesity induces a phenotypic switch in adipose tissue macrophage polarization. The Journal of clinical investigation. 2007;117(1):175-84.
18. Vroegrijk IO, van Klinken JB, van Diepen JA, van den Berg SA, Febbraio M, Steinbusch LK, et al. CD36 is important for adipocyte recruitment and affects lipolysis. Obesity. 2013;21(10):2037-45.
19. Weisberg SP, McCann D, Desai M, Rosenbaum M, Leibel RL, Ferrante AW, Jr. Obesity is associated with macrophage accumulation in adipose tissue. The Journal of clinical investigation. 2003;112(12):1796-808.
20. Kintscher U, Hartge M, Hess K, Foryst-Ludwig A, Clemenz M, Wabitsch M, et al. T-lymphocyte infiltration in visceral adipose tissue: a primary event in adipose tissue inflammation and the development of obesity-mediated insulin resistance. Arteriosclerosis, thrombosis, and vascular biology. 2008;28(7):1304-10.
21. Nishimura S, Manabe I, Nagasaki M, Eto K, Yamashita H, Ohsugi M, et al. CD8+ effector T cells contribute to macrophage recruitment and adipose tissue inflammation in obesity. Nature medicine. 2009;15(8):914-20.
22. Sackmann-Sala L, Berryman DE, Munn RD, Lubbers ER, Kopchick JJ. Heterogeneity among white adipose

tissue depots in male C57BL/6J mice. Obesity. 2012;20(1):101-11.

23. Marchesini G, Brizi M, Bianchi G, Tomassetti S, Bugianesi E, Lenzi M, et al. Nonalcoholic fatty liver disease: a feature of the metabolic syndrome. Diabetes. 2001;50(8):1844-50.
24. Strissel KJ, Stancheva Z, Miyoshi H, Perfield JW, 2nd, DeFuria J, Jick Z, et al. Adipocyte death, adipose tissue remodeling, and obesity complications. Diabetes. 2007;56(12):2910-8.
25. Wang QA, Tao C, Gupta RK, Scherer PE. Tracking adipogenesis during white adipose tissue development, expansion and regeneration. Nature medicine. 2013;19(10):1338-44.
26. Joe AW, Yi L, Even Y, Vogl AW, Rossi FM. Depot-specific differences in adipogenic progenitor abundance and proliferative response to high-fat diet. Stem cells. 2009;27(10):2563-70.
27. Jo J, Gavrilova O, Pack S, Jou W, Mullen S, Sumner AE, et al. Hypertrophy and/or Hyperplasia: Dynamics of Adipose Tissue Growth. PLoS computational biology. 2009;5(3):e1000324.
28. Skurk T, Alberti-Huber C, Herder C, Hauner H. Relationship between adipocyte size and adipokine expression and secretion. The Journal of clinical endocrinology and metabolism. 2007;92(3):1023-33.
29. Shimotsuma M, Shields JW, Simpson-Morgan MW, Sakuyama A, Shirasu M, Hagiwara A, et al. Morpho-physiological function and role of omental milky spots as omentum-associated lymphoid tissue (OALT) in the peritoneal cavity. Lymphology. 1993;26(2):90-101.
30. Hosogai N, Fukuhara A, Oshima K, Miyata Y, Tanaka S, Segawa K, et al. Adipose tissue hypoxia in obesity and its impact on adipocytokine dysregulation. Diabetes. 2007;56(4):901-11.
31. Rausch ME, Weisberg S, Vardhana P, Tortoriello DV. Obesity in C57BL/6J mice is characterized by adipose tissue hypoxia and cytotoxic T-cell infiltration. International journal of obesity. 2008;32(3):451-63.
32. Halberg N, Khan T, Trujillo ME, Wernstedt-Asterholm I, Attie AD, Sherwani S, et al. Hypoxia-inducible factor 1alpha induces fibrosis and insulin resistance in white adipose tissue. Molecular and cellular biology. 2009;29(16):4467-83.
33. Lumeng CN, DelProposto JB, Westcott DJ, Saltiel AR. Phenotypic switching of adipose tissue macrophages with obesity is generated by spatiotemporal differences in macrophage subtypes. Diabetes. 2008;57(12):3239-46.
34. Prieur X, Mok CY, Velagapudi VR, Nunez V, Fuentes L, Montaner D, et al. Differential lipid partitioning between adipocytes and tissue macrophages modulates macrophage lipotoxicity and M2/M1 polarization in obese mice. Diabetes. 2011;60(3):797-809.
35. Cannon B, Nedergaard J. Brown adipose tissue: function and physiological significance. Physiological reviews. 2004;84(1):277-359.
36. Harms M, Seale P. Brown and beige fat: development, function and therapeutic potential. Nature medicine. 2013;19(10):1252-63.
37. Townsend KL, Tseng YH. Brown fat fuel utilization and thermogenesis. Trends in endocrinology and metabolism: TEM. 2014;25(4):168-77.

ESM methods

Plasma parameters

At different time points during the HFD intervention blood was drawn from 6 hour fasted mice via the tail vein into paraoxon (Sigma, St. Louis, MO) coated capillary tubes to prevent ongoing *in vitro* lipolysis. After centrifugation, plasma was collected and glucose, insulin, triacylglycerol (TG), total cholesterol, and non-esterified fatty acid were determined using commercially available kits (Instruchemie, Delfzijl, The Netherlands; Crystal Chem Inc., IL, USA; 11488872 and 236691, Roche Molecular Biochemicals, Indianapolis; NEFA-C, Wako chemicals GmbH, Neuss, Germany, respectively).

Liver TG analysis

Lipids were extracted from livers according to a modified protocol from Bligh and Dyer (1). Briefly, small liver pieces were homogenized in ice-cold methanol. Lipids were extracted by addition of 1800 µl ice-cold chloroform/methanol (3:1) to 45 µl homogenate. The chloroform/methanol phase was dried and dissolved in 2% (vol./vol.) Triton X-100. Hepatic TG concentrations were measured using TG kit (11488872, Roche Molecular Biochemicals, Indianapolis). Liver TG were expressed per mg protein, which was determined using the BCA protein assay kit (Pierce Biotechnologie, Rockford, USA).

Adipocyte lipolysis assay

The potency of insulin to inhibit lipolysis in gonadal adipocytes was determined by incubating isolated adipocytes (±10,000 cells/ml) for 2 h at 37°C, with DMEM/F12 with 2% (vol./vol.) BSA and 8-bromo-cAMP (10^{-3} mol/l; Sigma, St. Louis, MO) in combination with or without insulin (10^{-9} mol/l). Glycerol concentrations were determined as a measure for lipolysis, using a free glycerol kit (Sigma, St. Louis, MO) and the hydrogen peroxide sensitive fluorescence dye Amplex Ultra Red, as previously described by Clark et al. (2).

Histology

Formalin fixed and paraffin embedded sections of gWAT and intrascapular BAT were used for histological analysis. An F4/80+ antibody (1:250) (Leiden University Medical Center, Leiden, The Netherlands) was used to stain macrophages in gWAT. Vectastain ABC (Vector laboratories, CA, US) was used for visualization of the antibody complex according to manufacturer's instructions. Haematoxylin staining of the gWAT and BAT sections was done using a standard protocol. The area of intracellular lipid vacuoles in BAT was quantified using Image J (NIH, US).

Flow cytometry analysis

Mouse SVF cells were stained with fluorescently labelled antibodies for CD45.2-FITC (BioLegend), CD3-APC, CD4-Qdot605, CD8a-PercpCy5.5, CD19-PE, F4/80-PE, CD11B-PB, CD11C-APCCy7 (all purchased from eBioscience, CA, USA or BioLegend, CA, USA). Cells were measured on a LSR II flow cytometer (BD Biosciences). Data were analysed using FlowJo software (Treestar, OR, USA).

Reference list

1. Bligh EG, Dyer WJ. A rapid method of total lipid extraction and purification. Canadian journal of biochemistry and physiology. 1959;37(8):911-7.
2. Clark AM, Sousa KM, Jennings C, MacDougald OA, Kennedy RT. Continuous-flow enzyme assay on a microfluidic chip for monitoring glycerol secretion from cultured adipocytes. Analytical chemistry. 2009;81(6):2350-6.

3

ESM figures and tables

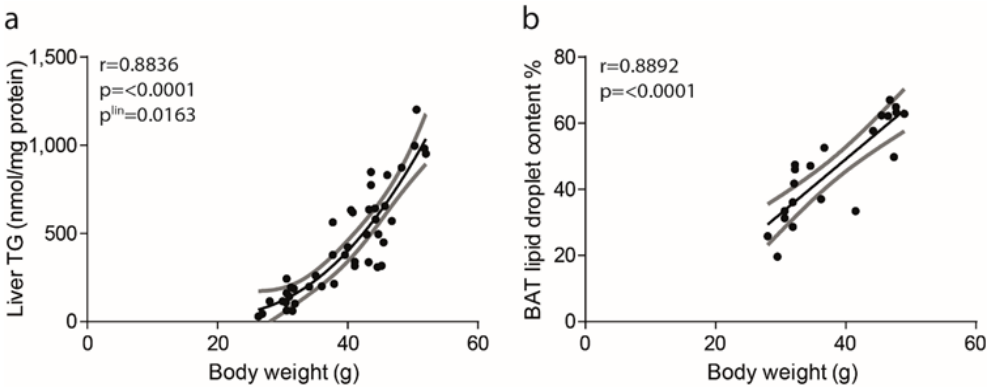

ESM Figure 1. Liver TG and BAT lipid droplet content. Liver TG content (A) and BAT lipid droplet content (B) are depicted per body weight. Associations were modelled using either a linear or non-linear function, 95% confidence interval is shown as grey bands. A significant value of *p* provides evidence of a non-zero slope in the linear model; a significant value of p^{lin} provides evidence that the association is non-linear.

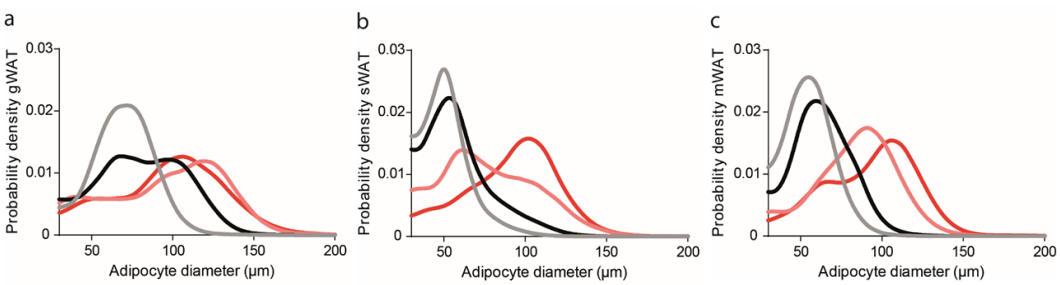

ESM Figure 2. Adipocyte size distributions with different body weights depicted per WAT depot. Mice were subdivided into different body weight groups; grey <30 grams, black 30-40 grams, pink 40-50 grams, red >50 grams. The mean adipocyte size distribution per group was depicted for the different WAT depots; gWAT (A), sWAT (B) and mWAT (C).

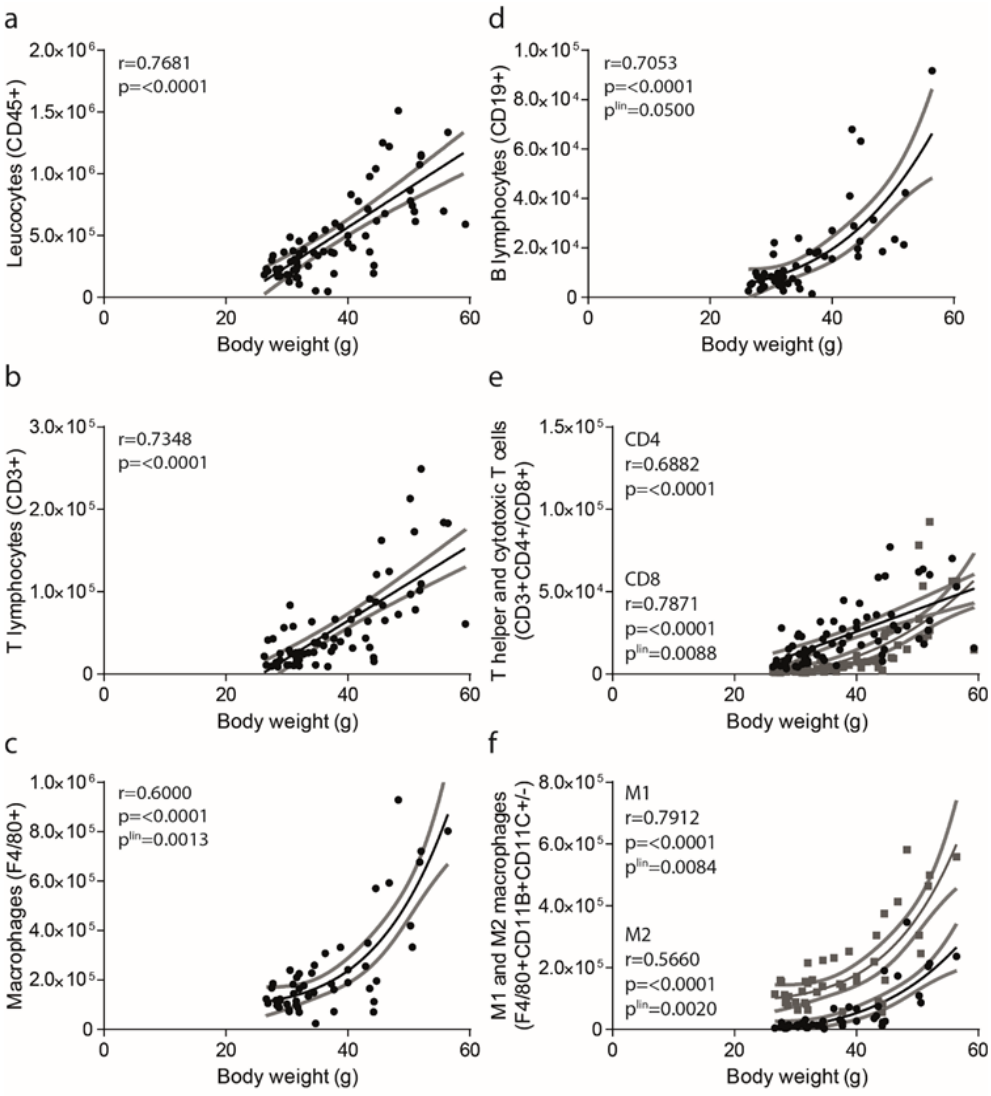

ESM Figure 3. Absolute immune cell numbers per fat pad of gonadal WAT correlated to body weight. Absolute numbers of leucocytes (A), T lymphocytes (B), macrophages (C), B lymphocytes (D), T helper (black dots) and cytotoxic T lymphocytes (grey squares) (E), and M1 (black dots) and M2 (grey squares) types of macrophages (F) are depicted per body weight. Associations were modelled using either a linear or non-linear function, 95% confidence interval is shown as grey bands. A significant value of *p* provides evidence of a non-zero slope in the linear model; a significant value of p^{lin} provides evidence that the association is non-linear.

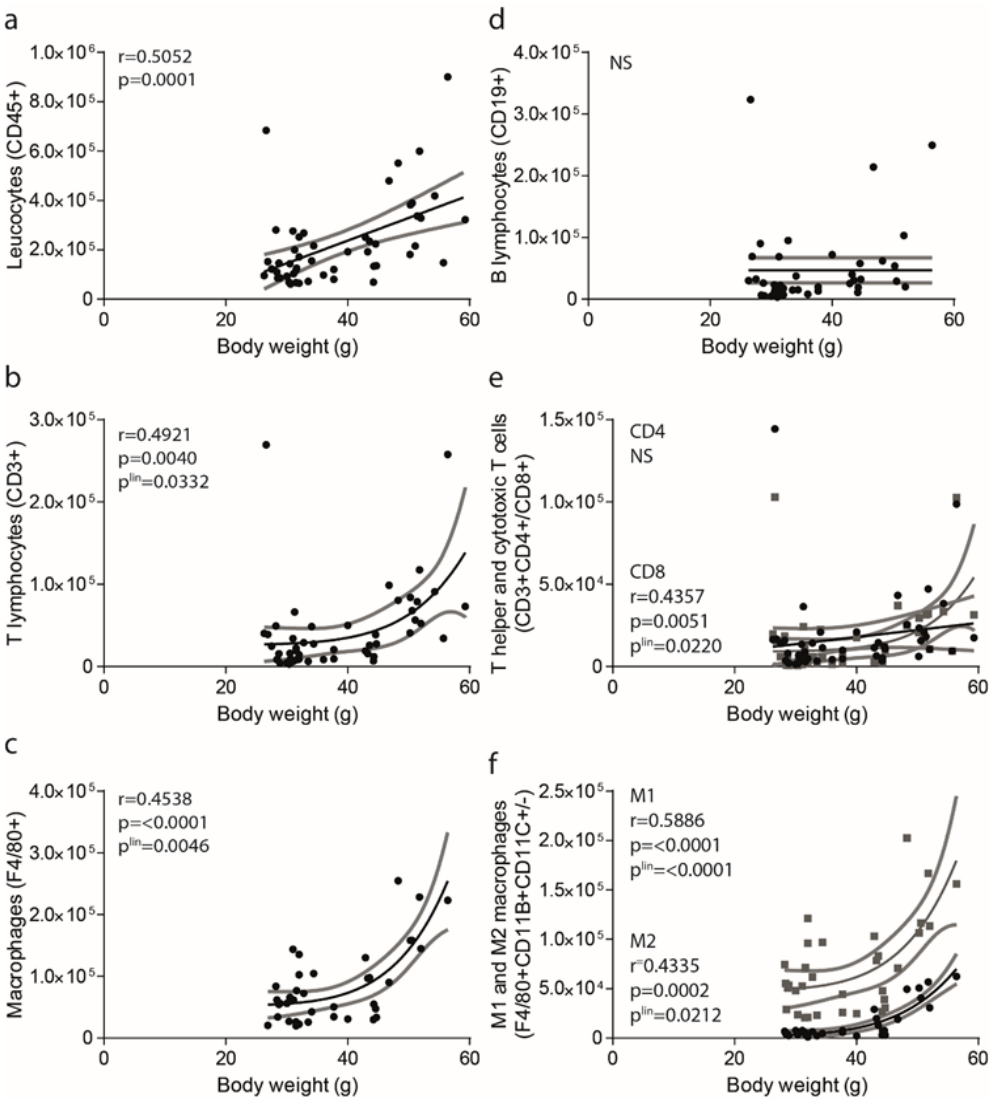

ESM Figure 4. Absolute immune cell numbers per fat pad of subcutaneous WAT correlated to body weight. Absolute numbers of leucocytes (A), T lymphocytes (B), macrophages (C), B lymphocytes (D), T helper (black dots) and cytotoxic T lymphocytes (grey squares) (E), and M1 (black dots) and M2 (grey squares) types of macrophages (F) are depicted per body weight. Associations were modelled using either a linear or non-linear function, 95% confidence interval is shown as grey bands. A significant value of *p* provides evidence of a non-zero slope in the linear model; a significant value of p^{lin} provides evidence that the association is non-linear.

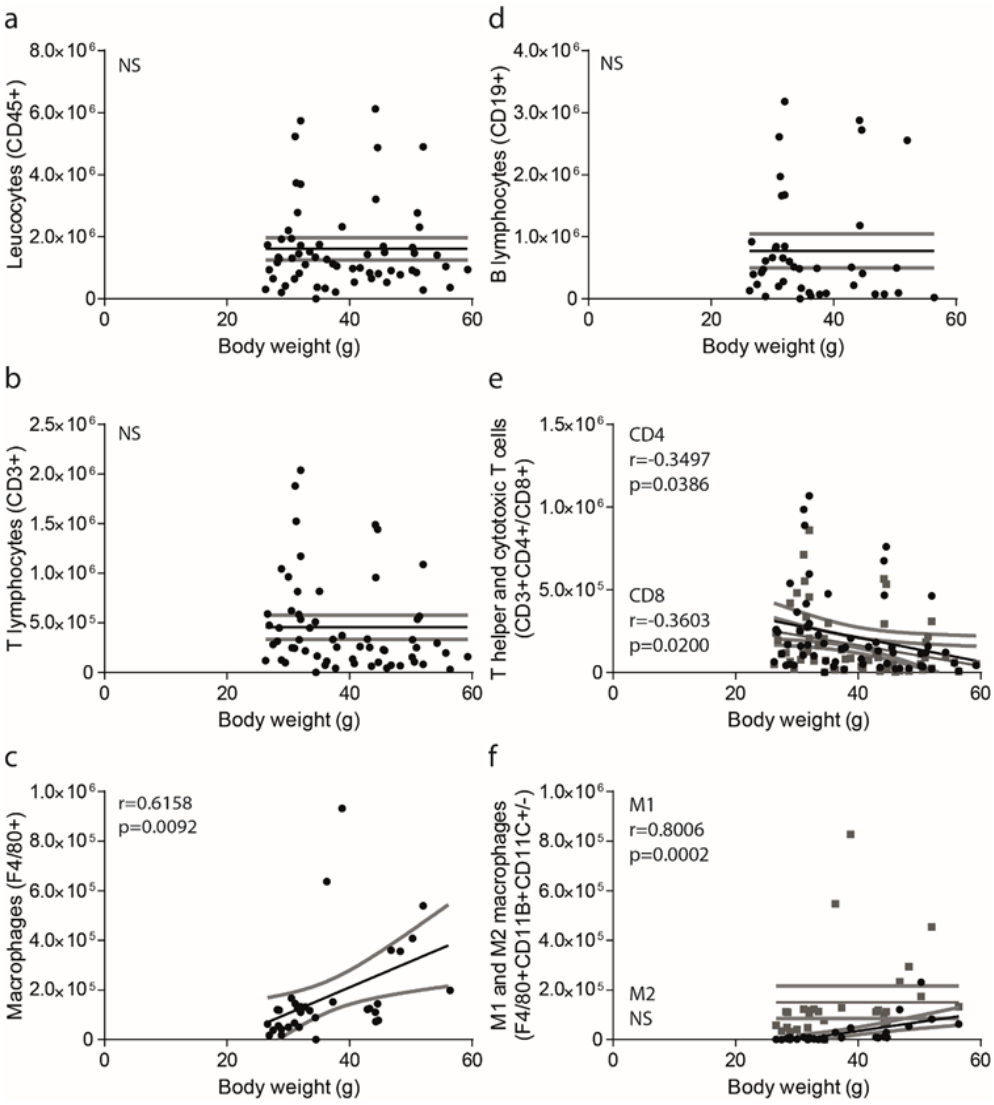

ESM Figure 5. Absolute immune cell numbers per fat pad of mesenteric WAT correlated to body weight. Absolute numbers of leucocytes (A), T lymphocytes (B), macrophages (C), B lymphocytes (D), T helper (black dots) and cytotoxic T lymphocytes (grey squares) (E), and M1 (black dots) and M2 (grey squares) types of macrophages (F) are depicted per body weight. Associations were modelled using either a linear or non-linear function, 95% confidence interval is shown as grey bands. A significant value of *p* provides evidence of a non-zero slope in the linear model; a significant value of p^{lin} provides evidence that the association is non-linear.

ESM Table 1. Batches of mice with different type and duration of diet intervention

Batch number	Weeks on diet	Type of diet	Number of animals (n)
1	4	45% HFD	10
2	8	45% HFD	10
3	11	45% HFD	9
4	34	45% HFD	8
5	5	60% HFD	9
6	15	60% HFD	8

ESM Table 2. Body composition and organ weight correlated to body weight of mice on a HFD

	Correlation to body weight - Statistics					
	a	**b**	**c**	***r***	***P*-value[a] zero slope**	***P*-value[a] linear**
Lean mass (g; n=36)	2.757	1.536e-004	20.60	0.9059	2.95E-15***	0.1206
Fat mass (g; n=36)	0.781	1.738	25.48	0.9517	7.75E-24***	0.1782
Liver weight (g; n=43)	5.123	3.160e-009	1.180	0.9424	3.94E-17***	3.12E-06***
Heart weight (g; n=26)	6.893	6.024e-014	0.1633	0.5734	2.70E-03**	0.1728
Spleen weight (g; n=35)	1	1.786e-003	0.0237	0.7271	5.07E-07***	1.000
BAT weight (g; 36)	1	0.01254	0.2645	0.9289	6.24E-16***	1.000
Gonadal FP weight[b] (g; n=54)	0.320	0.4411	26.21	0.7254	3.18E-11***	7.73E-04***
Subcutaneous FP weight[b] (g; n=54)	1	0.04113	-0.9205	0.9607	4.20E-26***	0.1620
Mesenteric FP weight (g; n=54)	1	0.0474	-1.084	0.8765	2.36E-20***	0.7785

Linear correlation: a=1; equation: $y=b \times x+c$

Non-linear power function with y-intercept: a>1; equation: $y=b \times x^a+c$

Non-linear power function with x-intercept: a<1; equation: $y=b \times (x-c)^a$

x=body weight; y=lean, fat or individual organ mass.

[a]*p*-value after bonferroni multiple test correction; **p*<0.05, ***p*<0.01, ****p*<0.001

[b]for gonadal and subcutaneous fat pad (FP) weight one of the two pads was used for calculations

ESM Table 3. Composition and comparison of WAT depots from lean mice

	Mouse WAT			Statistics[a]		
	gWAT (n=10)	sWAT (n=10)	mWAT (n=10)	T-test gWAT *vs* sWAT	T-test gWAT *vs* mWAT	T-test sWAT *vs* mWAT
Adipocyte size (µm)	97.8±13.2	77.0±13.1	71.3±11.8	0.0184*	0.0016**	1.000
Adipocyte no/ FP (*10^6)	2.03±0.70	2.81±0.98	2.69±0.59	0.4440	0.2912	1.000
SVF nr/FP (*10^6)	0.50±0.16	0.23±0.11	1.96±1.29	0.0024**	0.0192*	0.0040**
Leucocytes (% CD45 of SVF)	62.7±6.2	57.5±9.9	78.3±12.1	1.000	0.0184*	0.0088**
T lymphocytes (% CD3 of SVF)	7.5±2.2	14.2±8.9	27.5±10.2	0.2768	9.44E-05***	0.0744
T lymphocyte ratio (CD4:CD8)	5.1±2.3	1.54±0.66	1.29±0.36	0.0024**	8.00E-04***	1.000
B lymphocytes (% CD19 of SVF)	1.6±0.6	13.5±8.7	36.5±13.3	0.0032**	1.70E-06***	0.0040**
Macrophages (% F4/80 of SVF)	29.8±3.0	6.4±2.2	4.7±2.6	5.14E-06***	2.62E-05***	1.000

[a]*p*-value after bonferroni multiple test correction; *$p<0.05$, **$p<0.01$, ***$p<0.001$

ESM Table 4. Composition and comparison of WAT depots from obese mice

	Mouse WAT			Statistics[a]		
	gWAT (n=8)	sWAT (n=8)	mWAT (n=8)	T-test gWAT *vs* sWAT	T-test gWAT *vs* mWAT	T-test sWAT *vs* mWAT
Adipocyte size (µm)	124.4±8.0	112.0±2.5	113.9±5.5	0.0072**	0.0696	1.000
Adipocyte no/FP (*10^6)	2.10±0.36	3.02±0.47	3.41±0.84	0.0048**	0.0096**	1.000
SVF nr/FP (*10^6)	1.67±0.45	0.75±0.26	2.79±1.78	0.0016**	0.8328	0.0504
Leucocytes (% CD45 of SVF)	63.1±7.9	67.0±3.5	67.9±16.4	1.000	1.000	1.000
T lymphocytes (% CD3 of SVF)	6.6±2.0	12.5±4.2	11.3±9.4	0.0368*	1.000	1.000
T lymphocyte ratio (CD4:CD8)	1.15±0.47	1.00±0.24	1.77±0.56	1.000	0.3376	0.0280*
B lymphocytes (% CD19 of SVF)	2.1±1.2	13.0±10.2	19.3±21.2	0.1224	0.4192	1.000
Macrophages (% F4/80 of SVF)	37.5±3.9	6.5±1.8	17.9±10.5	7.69E-11***	0.0032**	0.0792

[a]*p*-value after bonferroni multiple test correction; *$p<0.05$, **$p<0.01$, ***$p<0.001$